A Journal of the Gesellschaft Deutscher Chemiker

Angewandte International Edition GDCh Chemie

www.angewandte.org

Accepted Article

Title: Inhibitor-induced dimerization of an essential oxidoreductase from African Trypanosomes

Authors: Annika Wagner, Thien Anh Le, Martha Brennich, Philipp Klein, Nicole Bader, Erika Diehl, Daniel Paszek, A. Katharina Weickhmann, Natalie Dirdjaja, R. Luise Krauth-Siegel, Bernd Engels, Till Opatz, Hermann Schindelin, and Ute A. Hellmich

To be cited as: *Angew. Chem. Int. Ed.* 10.1002/anie.201810470
Angew. Chem. 10.1002/ange.201810470

Link to VoR: http://dx.doi.org/10.1002/anie.201810470
http://dx.doi.org/10.1002/ange.201810470

WILEY-VCH

10.1002/anie.201810470

WILEY-VCH

COMMUNICATION

Inhibitor-induced dimerization of an essential oxidoreductase from African Trypanosomes

Annika Wagner,[a][b] Thien Anh Le,[c] Martha Brennich,[d] Philipp Klein,[e] Nicole Bader,[f] Erika Diehl,[a][b] Daniel Paszek,[a] A. Katharina Weickhmann,[b] Natalie Dirdjaja,[g] R. Luise Krauth-Siegel,[g] Bernd Engels,[c] Till Opatz,[e] Hermann Schindelin*[f] and Ute A. Hellmich*[a][b]

Abstract: Trypanosomal and leishmanial infections claim tens of thousands of lives each year. The metabolism of these single cell eukaryotic parasites differs from the human host and their enzymes thus constitute promising drug targets. Tryparedoxin (Tpx) from *Trypanosoma brucei* is the essential oxidoreductase in the parasite's hydroperoxide clearance cascade. Functional *in vitro* and *in vivo* assays show that a small, selective inhibitor efficiently inhibits Tpx. With X-ray crystallography, SAXS, analytical SEC, SEC-MALS, MD simulations, ITC, and NMR spectroscopy, we show how covalent binding of this monofunctional inhibitor leads to Tpx dimerization. Intra- and intermolecular inhibitor-inhibitor, protein-protein and inhibitor-protein interactions stabilize the dimer. The behavior of this efficient antitrypanosomal molecule thus constitutes an exquisite example of chemically induced dimerization with a small, monovalent ligand that can be exploited for future drug design.

Kinetoplastids, comprising African and South American Trypanosoma and Leishmania species, are the causative agents of devastating diseases. *Trypanosoma brucei* species cause human African Trypanosomiasis (African sleeping sickness), a neglected tropical disease, and Nagana cattle disease thus presenting a serious health risk as well as an economical threat. The essential oxidoreductase tryparedoxin (Tpx) in the *T. brucei* hydroperoxide clearance cascade, a distant relative of thioredoxins,[1] presents a promising drug target.[2] It undergoes thiol exchange reactions in its $WC_{40}PPC_{43}$ active site motif leading to peroxidase reduction and hydroperoxide clearance, protecting the parasite from oxidative damage (Scheme 1). The cascade also delivers reducing equivalents for DNA synthesis and protein repair, which are vital for pathogen metabolism and proliferation.[3]

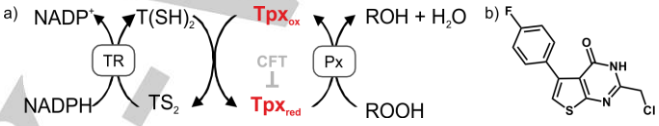

Scheme 1. (a) The *T. brucei* hydroperoxide clearance cascade consists of NADPH as the electron donor, trypanothione reductase (TR), trypanothione (TS_2/$T(SH)_2$), the oxidoreductase tryparedoxin (Tpx) and peroxidases (Px). CFT inhibits Tpx *in vitro* and *in vivo* (Fig. 1, Fig. S1). (b) Structure of the Tpx inhibitor CFT.[4]

A selective inhibitor (2-(chloromethyl)-5-(4-fluorophenyl)thieno[2,3-d]pyrimidin-4(3*H*)-one, **CFT**) for Tpx was previously described to covalently interact with C40 in the Tpx active site *in vitro* as well as *in vivo* (Fig. 1, S1).[4] In parasite cell culture, our EC_{50} data for CFT agree with previously published values (Fig. S1a).[4] Tpx activity and CFT inhibition efficiency were quantified *in vitro* via the rate of NADPH consumption in the reconstituted hydroperoxide clearance cascade (Scheme 1, Fig. S1b-d). Removing the chloride leaving group renders the inhibitor ineffective *in vivo* and *in vitro* (Fig. S1), thus highlighting the importance of the covalent interaction of CFT with Tpx.

To elucidate the structural basis of *T. brucei* Tpx inhibition, we studied the Tpx-CFT complex by X-ray crystallography, SAXS, MD simulations, analytical SEC, SEC-MALS, NMR and ITC and strikingly, found that CFT dimerizes Tpx.

"Small" molecules that promote chemically induced dimerization (CID), so called dimerizers, have been used, e.g. to control cellular signaling pathways.[5,6] Certain drugs, such as rapamycin, linking mTOR and FKBP, are naturally occurring heterodimerizers.[6] Covalently linked dimers of e. g. FK506 were used as artificial symmetric homodimerizers.[5] Most dimerizers tend to be relatively large and are almost always bifunctional.[5,6] In contrast, CFT presents a small, monofunctional dimerizer that covalently binds to Tpx.

Crystal structures exist of oxidized *T. brucei* Tpx as well as photo-reduced and glutathionylspermidine (a trypanothione mimic) bound *C. fasciculata* Tpx.[7] However, to date, no structure of a Tpx in complex with a drug molecule to serve as a starting point for structure-based drug design is available.

We thus determined the X-ray crystal structures of the *T. brucei* Tpx-CFT complex at 1.6 and 1.8 Å resolution (Fig. 1, Table S1). Each unit cell contains three chains, A. B and C, of the thioredoxin fold protein, each in complex with CFT (see SI for a more detailed description).

[a] A. Wagner, E. Diehl, D. Paszek, Prof. Dr. U. A. Hellmich
Institute of Pharmacy and Biochemistry
Johannes Gutenberg-University Mainz
Johann-Joachim-Becherweg 31, D-55128 Mainz, Germany
E-mail: u.hellmich@uni-mainz.de
[b] A. Wagner, A. K. Weickhmann, Prof. Dr. U. A. Hellmich
Biomolekulares Magnetresonanz Zentrum (BMRZ)
Goethe-Universität Frankfurt
Max-von-Laue Str. 9, D-60438 Frankfurt/M, Germany
[c] T.A. Le, Prof. Dr. B. Engels
Institute of Physical and Theoretical Chemistry
Julius-Maximilians-University Würzburg
Emil-Fischer-Straße 42, D-97074 Würzburg, Germany
[d] Dr. M. Brennich
Synchrotron Crystallography Team
EMBL Grenoble Outstation
71 Avenue des Martyrs, 38042 Grenoble, France
[e] P. Klein, Prof. Dr. T. Opatz
Institute of Organic Chemistry
Johannes Gutenberg-University Mainz
Duesbergweg 10-14, D-55128 Mainz, Germany
[f] N. Bader, Prof. Dr. H. Schindelin
Rudolf Virchow Center for Experimental Biomedicine
Julius-Maximilians-University Würzburg
Josef-Schneider-Straße 2, Haus D15, D-97080 Würzburg, Germany
E-mail: hermann.schindelin@virchow.uni-wuerzburg.de
[g] N. Dirdjaja, Prof. Dr. R. L. Krauth-Siegel
Biochemistry Center (BZH)
Ruprecht-Karls-University Heidelberg
Im Neuenheimer Feld 328, D-69120 Heidelberg, Germany

Supporting information for this article is given via a link at the end of the document.

10.1002/anie.201810470

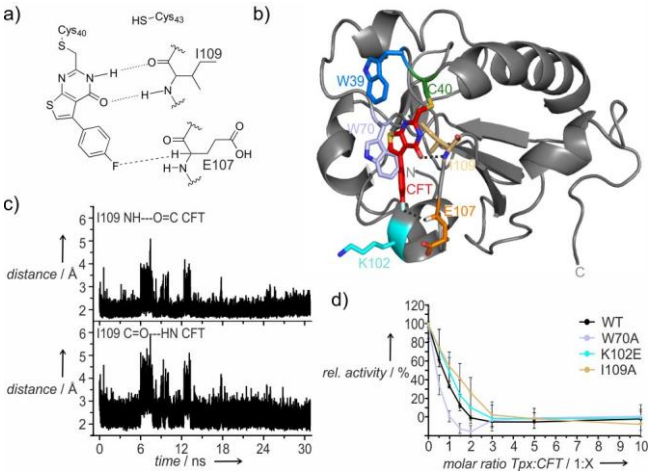

Figure 1. Structural basis of covalent inhibitor binding to Tpx. (a) Intramonomer CFT-Tpx contacts. (b) X-ray crystal structure of inhibitor-bound Tpx shows residues interacting with CFT intramolecularly. (K102 and W39 important for intermonomer interactions are also included (Fig. 2)). (c) MD simulations on Tpx-CFT monomer show stable interaction of CFT with I109 backbone atoms (mean distances are 2.1 ± 0.4 Å and 2.6 ± 0.6 Å). (d) Inactivation of Tpx variants after 5 min of Tpx:CFT co-incubation (5 µM Tpx final conc.) (basal activities in Fig. S2).

Chains A and B of the 1.6 and 1.8 Å Tpx WT (wild type) structures are very similar to each other within and across data sets (Table S2, Fig. S3). The bound inhibitor orientation with respect to the active site is identical in all four copies. In contrast, chain C in both data sets shows CFT in a different conformation and exhibits higher mobility than chains A and B. The different CFT orientation leads to conformational changes in residues 70-75 and 91-109.
In chains A and B, the CFT molecule is embedded in a pocket created by W39, W70 and I109 (Fig. 1). The I109 side chain packs against the surface of the CFT thienopyrimidone via hydrophobic interactions. The I109 backbone amide forms a weak hydrogen bond with the inhibitor's carbonyl group (N-O distance of 3.4 Å). This interaction is also preserved in MD simulations of the monomeric Tpx-CFT complex (Fig. 1). Further CFT interactions and positioning are due to the T-shaped π-stacking of the W70 side chain with CFT's ring system. W39, next to C40, seems to have less of an intramonomer stabilizing influence on the inhibitor, but plays an important role in intermonomer stabilization (see below). Finally, Hα of E107, a weak hydrogen bond donor, interacts with the CFT fluoride, a strong hydrogen bond acceptor. This interaction is also observed in our MD simulation (Fig. S4).

Chains A and B of our X-ray crystal structures form a C_2 symmetric parallel homodimer with two CFT molecules sandwiched between them (Fig. 2). Interactions across the Tpx-CFT dimer interface include stacking of the W39' indole ring with the inhibitor's methylene group covalently connected to C40 of the opposite chain and an intermolecular salt bridge zipper between the side chains of K102/E107' and K102'/E107, thus closing off the inhibitor binding site (Fig. S3). Accordingly, these side chains stably interact in MD simulations of the Tpx dimer (Fig. S4). CFT-CFT' interactions across the dimer interface are mediated through extensive π-π-stacking between the thienopyrimidone ring systems and lone pair-π interactions between the thiophene sulfur atoms and the pyrimidone rings (Fig. 2).[8] The latter interaction has recently gained increasing recognition in biological systems, in the structural properties of drugs as well as for the rational design of bioorganic catalysts.[9,10]
In the Tpx_2-CFT_2 complex, 1870 Å^2 of surface area are buried (563/573 Å^2 for Tpx monomers and 368/364 Å^2 for inhibitors) corresponding to 12.5% of the total surface area of 14950 Å^2 indicating that dimerization should be stable in solution. Remarkably, almost the complete surface area (90/89%) of the two CFT molecules is buried upon dimer formation illustrating almost total integration into the Tpx dimer interface (Fig. S3).

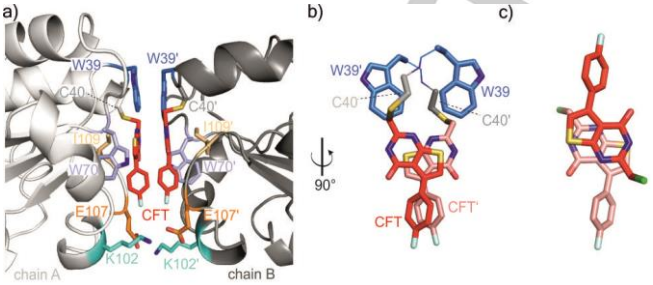

Figure 2. Tpx dimer interface. (a) Crystallographically observed inhibitor-mediated dimerization interface. Residues K102/E107' and E107/K102' (cyan, orange) form intermolecular salt bridges. W70 (lilac) and I109 (tan) contact CFT intramolecularly. (b) Tpx-bound CFT molecules (red) stack in parallel. The W39/W39' side chains (blue) interact with CFT across the dimer interface. To clearly demonstrate intermonomer protein-inhibitor and inhibitor-inhibitor interactions, the main chain between W39/W39' and C40/C40' is shown with thin lines. (c) Crystal packing of CFT in isolation shows an antiparallel orientation (Table S3, Fig S5). Non-carbon atom color scheme: blue: N, red: O, yellow: S, cyan: F, green: Cl.

To probe whether CFT-induced Tpx dimerization indeed occurs in solution, we carried out analytical size exclusion chromatography (SEC), small angle X-ray scattering (SAXS) and NMR spectroscopy (Fig. 3, S6, S7 Table S4). In the SEC experiments, Tpx WT readily dimerizes in the presence of CFT. In the SAXS data, Tpx-CFT appears slightly smaller than expected for the crystallographic dimer (expected radius of gyration 2.2 nm), but can be described very well as a mixture of the crystallographic monomer and dimer. Independently, *ab initio* models for a monomer-dimer mixture align very well with the crystallographic models (Fig. 3).[11] Dimer formation also explains the extensive line broadening observed in ^{1}H, ^{15}N-HSQC spectra of Tpx-CFT (Fig. 3, S7). Tpx dimerization at a ~1:1 molar ratio of Tpx to CFT is a consequence of the covalent nature of the inhibitor and indicates high affinity for the protein-inhibitor complex dimer. SEC measurements of Tpx-CFT after 24 h did not show a recurrent increase in monomer (Fig. S8) suggesting long-term stability of the complex. The K_D for the dissociation of the Tpx-CFT dimer is 5.7 ± 1.4 µM as determined by dilution isothermal titration calorimetry (ITC) (Fig. 4, S9).[12] Since we did not observe any signs of Tpx dimerization in the absence of CFT, even at high protein concentrations, this shows that the inhibitor is essential for inducing Tpx dimerization in solution.

Next, we probed the molecular determinants for Tpx dimerization, beginning with CFT itself. Tpx does not dimerize in the absence of CFT and Tpx-bound CFT shows a parallel orientation. In contrast, isolated CFT crystallizes in an antiparallel stacking mode (Fig. 2, S5, Table S3), thus indicating that CFT stacking alone is not sufficient to drive Tpx dimerization. Nonetheless, our X-ray crystal structures in combination with MD simulations support the notion that it contributes significantly to dimer stability. When comparing Tpx monomer dynamics in the absence and presence of CFT in MD simulations, the mean RMSD values significantly decrease with CFT (Fig. 3). Upon removal of the CFT molecules from Tpx in a simulation of the dimer, the intermolecular salt bridge between K102 and E107' (K102'/E107) across the dimer interface is lost and Tpx chain RMSD values increase compared to the CFT-bound protomers (Fig. S4), further supporting the notion that CFT is necessary not only to induce but also to stabilize the Tpx dimer and also indicating that additional

10.1002/anie.201810470

interactions of amino acids across the Tpx dimer interface are important for dimer stabilization.

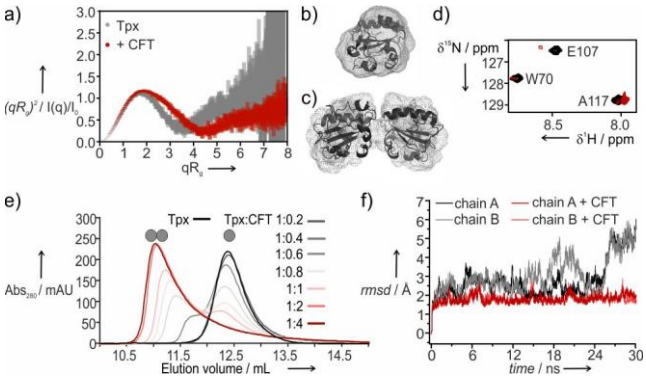

Figure 3. Tpx dimerizes in solution. (a) Kratky plots of Tpx WT (grey) and in the presence of CFT (red) (compare Fig. S6). (b, c) Envelopes modelled on SAXS data show good agreement with monomer and dimer from our crystal structure. (d) ^{1}H, ^{15}N-HSQC spectrum of reduced Tpx (black) and CFT-induced line broadening (red) (Fig. S7). (e) Tpx dimerization starts at sub-stoichiometric Tpx:CFT ratios in analytical SEC. (f) Tpx dimer (black) is stabilized by CFT binding (red) in MD simulations. RMSD values (relative to initial chain position) for chains A and B with CFT are 1.8 ± 0.2 Å and 1.9 ± 0.2 Å, respectively. Without CFT, RMSD values increase to 2.8 ± 0.9 Å and 3.1 ± 1.0 Å.

To elucidate the role of individual amino acids for Tpx dimerization, point mutations at positions interacting with CFT in our X-ray crystal structure or playing a role in the MD simulations (W39, C40, W70, K102, I109) were introduced. None of the substitutions compromised Tpx structural integrity as shown by CD spectroscopy, SEC and SAXS (Fig. S2, S6, S8, Table S4). Their enzymatic activity was measured in the peroxidase assay (Scheme 1, Fig. 1d, Fig. S2). As expected, mutating the active site (Tpx C40S or C43S) led to inactive protein. Tpx W39A, W70A and I109A retained 2.3 ± 0.8%, 21.6 ± 1.9% and 32.4 ± 1.5% of WT activity, respectively, whereas Tpx K102E displayed an enhanced activity (159.6 ± 12.2%) (Fig. S2). We also tested inhibition and covalent inhibitor interaction for all Tpx variants. CFT efficiently inhibited the Tpx variants (Fig. 1d). For Tpx W39A, the basal activity was so low that no further inhibition by CFT could be measured. Tpx W70A was more efficiently inhibited than WT (Fig. 1d, S2). This may potentially reflect a diminished steric hindrance for CFT binding upon removal of the bulky indole ring. Reaction of maleimide-PEG with available cysteine residues leads to an increase in molecular size of Tpx. Pre-incubation with CFT blocks C40 when a covalent complex is formed. Analysis by SDS-PAGE confirmed that all Tpx variants except C40S covalently bind CFT (Fig. 4e).

Since we established that the Tpx mutations do not compromise structural integrity or CFT interaction, we next probed their ability to dimerize by analytical SEC and SAXS. Tpx W70A and I109A behave as the WT with CFT, while the W39A mutant does not dimerize (Fig. S6, S8). For Tpx K102E, a radius of gyration intermediate between monomer and dimer indicated that dimerization was only partially abrogated (Fig. 4b), in agreement with MD simulations showing that the intermolecular salt bridge between K102/E107' and K102'/E107 is transient (Fig. S4). We thus compared ITC and SEC-MALS (SEC multiangle light scattering) data of Tpx WT with Tpx W39A and K102E (Fig. 4, S9, S10). As expected, in SEC-MALS, Tpx WT shifts to higher molecular weight with CFT, but Tpx W39A does not. For Tpx K102E, an intermediate molecular weight is observed. Our ITC measurements confirmed that CFT-complexed Tpx W39A does not dimerize and that the K_D for dimerization of K102E-CFT is about 15-fold higher (83.1 ± 32.2 µM) than that of the WT. Concurrently, at high protein concentrations (400 µM), Tpx K102E-CFT dimerizes on analytical SEC, but W39A does not, even at concentrations of 850 µM (Fig. S8). Intermolecular salt bridge formation is thus an important, yet secondary determinant for inhibitor-dependent Tpx dimerization, while the W39-CFT interaction across the dimer interface is essential.

Our data reveal essential interactions for CFT-induced dimerization of Tpx: (i) inhibitor-inhibitor interactions mediated by the parallel stacking of two CFT molecules and (ii) intermolecular protein-inhibitor interactions through the W39 sidechains. Dimer formation is further promoted by (iii) the salt bridges formed between K102 and E107 of opposing Tpx monomers. Removal of any of these components results in a complete or partial breakdown in dimerization. Importantly, formation of this set of molecular interactions is strictly inhibitor-dependent and thus readily inducible upon addition of CFT to Tpx.

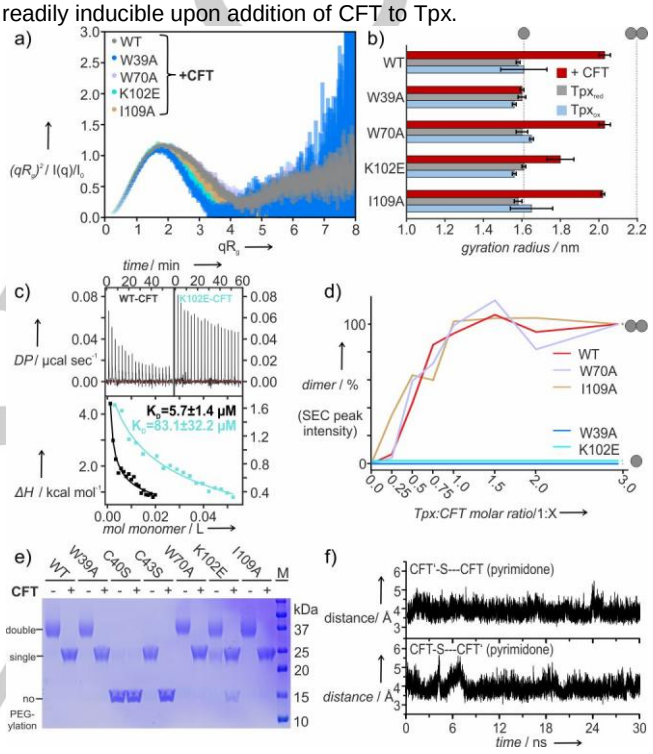

Figure 4. Molecular determinants of inhibitor-induced Tpx dimerization. Kratky plots of Tpx variants in complex with CFT (Fig. S6). (b) Radii of gyration for Tpx variants. All proteins are monomeric in the oxidized (blue) and reduced (grey) states. CFT addition increases radii of gyration for Tpx WT, W70A and I109A (and partially for K102E). (c) Dissociation ITCs for Tpx WT-CFT and K102E-CFT (top: raw data; bottom: integrated heat signatures and fitted curves). (d) Analytical SEC shows CFT-dependent Tpx dimer formation for WT, W70A and I109A, but not W39A and K102E (100 µM protein/run) (Fig. S8). (e) Maleimide-PEG assay probes PEGylation at C40 and C43. CFT binding blocks C40. The SDS-PAGE shows that all Tpx variants except C40S interact with CFT (4 µg protein/lane). (f) MD simulation of the Tpx dimer shows stable interactions between CFT molecules. The mean distances between the CFT sulfur and the geometrical center of CFT' pyrimidone and *vice versa* (3.9 ± 0.4 Å; 3.9 ± 0.3 Å) are typical for lone pair-π -interactions.[9]

In summary, we establish the structural basis for CFT-Tpx interaction furthering antitrypanosomal drug development and show how a monofunctional, small molecule induces stable protein dimerization, enabled by intra- and intermonomer interactions, thus extending the available framework for CID. Potential drawbacks regarding limited affinity compared to prototypical dimerizers can be overcome by the covalent irreversible nature of inhibitor binding to the target molecule.[13] This is a novel concept that may be exploited in rational drug design for other proteins in the future.

Experimental Section

Tpx-CFT X-ray crystal structure coordinates (PDB: 6GXG, 6GXY), SAXS data (SASBDB: SASDEY3, -Z3, -24, -34, -44, -54, -64, -74, -84, -94, -A4, -B4, -C4, -D4, -E4, -F4, -G4, -H4, -J4) and Tpx_{ox}/Tpx_{red} NMR assignments (BMRB: 27049, 27050)[11] are available. CCDC 1862408 contains the supplementary crystallographic data for isolated CFT. These data are provided free of charge by the Cambridge Crystallographic Data Centre. *T. brucei in vivo* and *in vitro* functional assays, SAXS, SEC, X-ray crystal structure determination, ITC, CD and NMR spectroscopy and CFT synthesis are described in Supplementary Material.

Acknowledgements

We acknowledge support by the Carl Zeiss Foundation, the JGU Mainz Inneruniversitäre Forschungsförderung (to UAH), the Rudolf Virchow Center for Experimental Biomedicine of Würzburg University (to HS), the Rhineland-Palatinate Natural Products Research Center and the Center for Biomolecular Magnetic Resonance (BMRZ), Frankfurt University funded by the state of Hesse. AW thanks the Prof. Rochelmeyer Stiftung for a travel stipend. ED acknowledges a TransMED – Mainz Research School of Translational Biomedicine PhD fellowship. We acknowledge Dres Liermann, Kampf and Schollmeyer for CFT NMR spectroscopy, MS and CFT crystal structure analysis, S. Jung for discussions and Dr. Kasaragod for MX data collection and help with MALS experiments and ESRF (beamlines ID29, ID23-1, BM29) and BESSY II (beamline 14.1) for synchrotron radiation facilities and beamline staff for assistance.

Keywords: Oxidoreductase • African Trypanosomes • chemically induced dimerization (CID) • Tryparedoxin • covalent inhibitor

[1] H. Lüdemann, M. Dormeyer, C. Sticherling, D. Stallmann, H. Follmann, R.L. Krauth-Siegel, *FEBS Lett* **1998**, *431*, 381.
[2] M. A. Comini, R. L. Krauth-Siegel, L. Flohé, *Biochem J* **2007**, *402*, 43.
[3] a) A. E. Leroux, R. L. Krauth-Siegel, *Mol Biochem Parasit* **2016**, *206*, 67; b) B. Manta, M. Bonilla, L. Fiestas, M. Sturlese, G. Salinas, M. Bellanda, M. A. Comini, *Antioxid Redox Sign* **2018**, *28*, 463.
[4] F. Fueller, B. Jehle, K. Putzker, J. D. Lewis, R. L. Krauth-Siegel, *J Biol Chem* **2012**, *287*, 8792.
[5] D. Spencer, T. Wandless, S. Schreiber, G. Crabtree, *Science* **1993**, *262*, 1019.
[6] S. Voß, L. Klewer, Y.-W. Wu, *Curr opin Chem Bio* **2015**, *28*, 194.
[7] a) M. S. Alphey et al., *J Biol Chem* **2003**, *278*, 25919; b) B. Hofmann et al., *Biol Chem* **2001**, *382*, 459.
[8] M. Egli, S. Sarkhel, *Accounts Cem Res* **2007**, *40*, 197.
[9] M. Chawla, E. Chermak, Q. Zhang, J. M. Bujnicki, R. Oliva, L. Cavallo, *Nucleic Acids Res* **2017**, *45*, 11019.
[10] A. J. Neel, M. J. Hilton, M. S. Sigman, F. D. Toste, *Nature* **2017**, *543*, 637.
[11] A. Wagner, E. Diehl, R. L. Krauth-Siegel, U. A. Hellmich, *Biomol NMR Assign* **2017**, *11*, 193.
[12] a) H. R. Broom, J. A. O. Rumfeldt, K. A. Vassall, E. M. Meiering, *Protein Sci* **2015**, *24*, 2081; b) S. D. Burrows et al., *Biochemistry* **1994**, *33*, 12741.
[13] a) S. Previti et al., *J Med Chem* **2017**, *60*, 6911; b) T. Schirmeister et al., *J Am Chem Soc* **2016**, *138*, 8332.

10.1002/anie.201810470

WILEY-VCH

COMMUNICATION

Chemically induced dimerization usually requires large, bifunctional molecules. In their communication, Wagner et al provide a high-resolution view how a small, covalent, monovalent inhibitor efficiently induces dimerization of an essential oxidoreductase from the parasite *Trypanosoma brucei*, the agent causing African Sleeping Sickness, through elaborate intra- and intermolecular interactions.

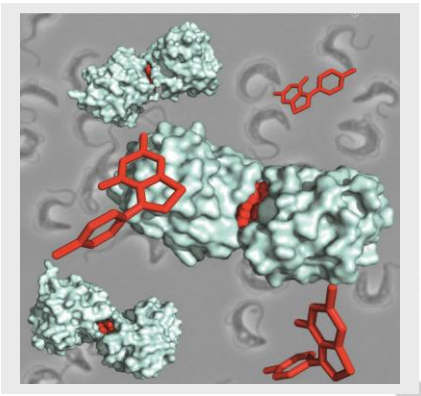

Annika Wagner, Thien Anh Le, Martha Brennich, Philipp Klein, Nicole Bader, Erika Diehl, Daniel Paszek, A. Katharina Weickhmann, Natalie Dirdjaja, R. Luise Krauth-Siegel, Bernd Engels, Till Opatz, Hermann Schindelin and Ute A. Hellmich**

Page No. – Page No.
Inhibitor-induced dimerization of an essential oxidoreductase from African Trypanosomes